Title: Light-driven Water Splitting Mediated by Photogenerated Bromine

Authors: Matthew Vincent Sheridan, PhD; Ying Wang; Degao Wang; Ludovic Troian-Gautier; Christopher J Dares; Benjamin D Sherman; Thomas J Meyer

To be cited as: 10.1002/anie.201708879

Link to VoR: https://doi.org/10.1002/anie.201708879

Light-driven Water Splitting Mediated by Photogenerated Bromine

Matthew V. Sheridan,* Ying Wang, Degao Wang, Ludovic Troian-Gautier, Christopher J. Dares, Benjamin D. Sherman, and Thomas J. Meyer

Abstract: *Light-driven water splitting was achieved using a dye-sensitized mesoporous oxide film and the oxidation of bromide (Br^-) to bromine (Br_2) or tribromide (Br_3^-). The chemical oxidant (Br_2 or Br_3^-) is formed during illumination at the photoanode and used as a sacrificial oxidant to drive a water oxidation catalyst (WOC), here demonstrated using [Ru(bda)(pic)$_2$], (**1**, pic = picoline, bda = 2,2'-bipyridine-6,6'-dicarboxylate). The photochemical oxidation of bromide produces a chemical oxidant with a potential of 1.09 V vs NHE for the Br_2/Br^- couple or 1.05 V vs NHE for the Br_3^-/Br^- couple sufficient to drive water oxidation at **1** ($Ru^{V/IV}$ = ~1.0 V vs NHE at pH 5.6). At pH 5.6, using a 0.2 M acetate buffer containing 40 mM LiBr and the [Ru(4,4'-PO_3H_2-bpy)(bpy)$_2$]$^{2+}$ (**RuP**$^{2+}$, bpy = 2,2'-bipyridine) chromophore dye on a SnO_2/TiO_2 core-shell electrode, resulted in a photocurrent density of ~1.2 mA/cm^2 under ~1 Sun illumination and a Faradaic efficiency upon addition of **1** of 77% for oxygen evolution.*

Water splitting ($2H_2O \rightarrow O_2 + 2H_2$) is one of the many approaches under investigation for alleviating the world's dependence on fossil fuels.[1, 2] Light-driven water splitting to generate solar fuels is particularly attractive since it mimics Nature's photosynthetic scheme and harnesses an abundant and cost-free energy source, sunlight.[3] Water oxidation typically presents the greatest challenge of the contributing half reactions in water splitting due to the $4e^-$ chemistry and need for high oxidation potentials to carry out the reaction: $2H_2O \rightarrow O_2 + 4H^+ + 4e^-$; E^o = 1.23 V versus NHE. This challenge limits the availability of rapid and stable molecular catalysts for use in devices based on a photoanode and dark cathode, in devices such as the one described here.[4, 5] Photoanodes perform water oxidation with solar energy and—when paired with an appropriate semiconductor—carry out water or CO_2 reduction at the cathode. This latter half reaction provides hydrogen ($2H^+ + 2e^- \rightarrow H_2$; E^o = 0.0 V versus NHE) or a reduced form of carbon as the solar fuel. Alternatively, devices based on a photocathode and dark anode are limited by cheap and effective semiconductors.[6, 7]

An attractive approach for carrying out light-driven water splitting is with a dye-sensitized photoelectrochemical cell (DSPEC).[8, 9] The DSPEC typically consists of a chromophore and catalyst assembly attached to a semiconductor forming the photoanode, a dark cathode (typically Pt), and an ion selective membrane separating the two electrodes that are wired together. Immobilization of the water oxidation catalyst (WOC) alongside the chromophore allows for hole transfer from the ground-state oxidized chromophore (following electron injection into the semiconductor) to the catalyst. This is a process that must occur four times in order for water oxidation to occur. The demand for four oxidative equivalents to build-up at the catalyst puts a heavy demand on the dynamics of charge separation at the semiconductor. The concentration of oxidative charge at the catalyst both decreases the driving force for subsequent hole transfers from the photo-oxidized dye as well as increases the driving force for charge recombination from electrons in the semiconductor. In order to facilitate longer charge separation lifetimes, a number of techniques have been developed to both alter the arrangement of the chromophore and catalyst at the surface and to alter the properties of the semiconductor.[10, 11] A promising technique is to construct core-shell electrodes using two different semiconductor materials, such as SnO_2 and TiO_2.[12-14] Electrodes constructed in this way, with a more insulating (more negative conduction band) oxide as the shell, are generally *ca.* 10 times more efficient in converting light energy into photocurrent and O_2.[15, 16]

In this report, in order to avoid the buildup of oxidative charge at the photoanode surface, an electron-transfer mediator has been employed using the Br^-/Br_2 couple (E = 1.09 V versus NHE) or Br^-/Br_3^- couple (E = 1.05 V versus NHE).[17] Oxidation of bromide, Br^-, to either product provides an oxidant capable of driving water oxidation at an added [Ru(bda)(L)$_2$] (bda is 2,2'-bipyridine-6,6'-dicarboxylate) catalyst with L a neutral donor ligand such as pyridine.[18] [Ru(bda)(L)$_2$] catalysts used here typically have Ru(V/IV) redox couples *ca.* 1 V versus NHE at or above pH 5.5.[19, 20] This is the highest potential in the water oxidation cycle for these catalysts and one that should be thermodynamically accessible with bromine/tribromide as an outer-sphere oxidant ([Ru^{IV}=O] + *oxidized bromide species* → [Ru^{V}=O] + Br^-). In related halogen oxidations, additional halogenated intermediates have been invoked as participants.[21] Bromine will be referenced throughout because it is known to have the fastest electron transfer kinetics and is in rapid equilibrium with the other oxidized bromide species (for instance, tribromide). The results of studies described below demonstrate that both oxidants support water oxidation catalysis by [Ru(bda)(L)$_2$] catalysts. The complex sodium bromine acetate-tribromide ([$CH_3CO_2Br\{Br_3\}$][Na]) was found to be the predominant product in solution following the photochemical oxidation of bromide *vida infra*. This complex is formed from the reaction of two bromine molecules with acetate ($2Br_2 + CH_3CO_2^- \rightarrow [CH_3CO_2Br\{Br_3\}]^-$). In order to perform water oxidation with *bromine*, a [Ru(bda)(L)$_2$] complex was added to solution following photolysis to complete the light-driven water splitting cycle (Scheme 1).

[*] M. V. Sheridan, Prof. C. J. Dares
Department of Chemistry and Biochemistry
Florida International University
Modesto Maidique Campus, CP304 - 11200 SW 8th St. Miami, Florida 33199
E-mail: msherida@fiu.edu
D. Wang, Y. Wang, L. Troian-Gautier, Prof. T. J. Meyer
Department of Chemistry
University of North Carolina at Chapel Hill
Campus Box 3290
Chapel Hill, NC 27599-3290
B. D. Sherman
Department of Chemistry
Texas Christian University
TCU Box 298860
Fort Worth, Texas 76129

Supporting information for this article is given via a link at the end of the document.

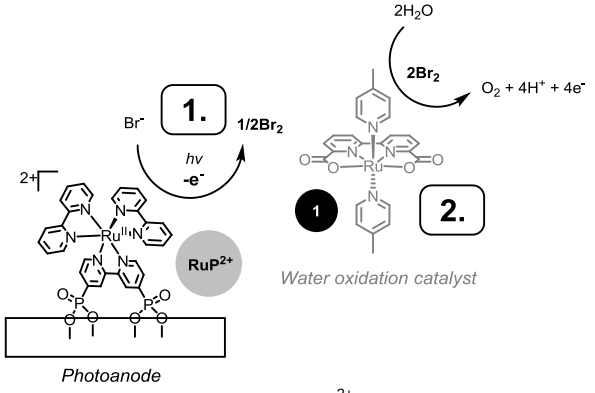

Scheme 1. Structure of the **RuP**$^{2+}$ chromophore and water oxidation catalyst **1** and the (photo)chemical steps leading to water oxidation: 1) light absorption by **RuP**$^{2+}$, charge separation forming **RuP**$^{3+}$, and Br^- oxidation by **RuP**$^{3+}$ to form $1/2Br_2$ and 2) oxidative consumption of the photochemically formed Br_2 resulting in water oxidation by **1** in solution.

The electrochemistry of Br^- under aqueous conditions is summarized in Eqn 1-4.[17] Two noteworthy aspects are the small equilibrium constant between Br_2 and Br_3^- in the presence of Br^- (K_{eq} = 17)[22] and the more rapid ET kinetics of Br_2 with the electrode surface.[23] The formation constant (K_{eq}) for Br_3^- is significantly lower than that of triiodide in water (I_3^-, K_{eq} = 698)[24] or for the same reaction to form tribromide in nonaqueous solvents ($K_{eq} > 10^6$).[25] Along with the faster ET kinetics known for Br_2, the small equilibrium constant for Br_3^- formation could inhibit Br_2/Br_3^--Br^- couple as a redox mediator. Recombination of Br_2 with the reduced oxide surface under illumination would result in poorer overall photocurrent efficiencies.

$$3Br^- \rightarrow Br_3^- + 2e^- \quad E^o = 1.05 \text{ V versus NHE} \quad (1)$$

$$2Br^- \rightarrow Br_2 + 2e^- \quad E^o = 1.09 \text{ V versus NHE} \quad (2)$$

$$Br_3^- \leftrightarrow Br_2 + Br^- \quad K_{eq} = 17 \quad (3)$$

$$Br_2 + 2e^- \rightarrow 2Br^- \quad \textit{rapid} \quad (4)$$

$$2TiO_2(e^-) + Br_2 \rightarrow TiO_2(0) + 2Br^- \quad \textit{recombination} \quad (5)$$

To test for the photoelectrochemical oxidation of bromide in water, a phosphonated derivative of the ruthenium *tris*-bipyridine dication, **RuP**$^{2+}$ ([Ru(4,4'-H_2O_3P-bpy)(bpy)$_2$]$^{2+}$), was used on TiO_2 and SnO_2/TiO_2 core-shell electrodes in aqueous media at pH 1 and pH 5.6. Recent results in this area have shown that ruthenium *tris*-bipyridine dyes are competent chromophores for the oxidation of bromine in nonaqueous media.[26-28] The core-shell electrode configuration was used here in anticipation of the slower ET rate between **RuP**$^{3+}$ (formed following excited state injection, $E_{1/2}$ = 1.26 V versus NHE) and Br^- ($E_{1/2}$ = 1.05-1.09 V versus NHE).[29] The longer charge separation lifetimes provided by the core-shell electrodes have resulted in enhanced photocurrent efficiencies which in some cases are a >10-fold enhancement over traditional TiO_2 electrodes.[15] This has been critical to improving photocurrent efficiencies observed in water splitting devices where heterogeneous water oxidation rates are rate limiting.[30]

Figure 1 reveals the results of experiments on **RuP**$^{2+}$ electrodes in solutions containing 40 mM LiBr at pH 1 and pH 5.6 in a 0.2 M acetate buffer. The SnO_2/TiO_2 electrodes performed better in both solutions with photocurrent densities of 1.2 mA/cm^2 and 0.25 mA/cm^2 at pH 5.6 and pH 1, respectively. This comparison suggests that the reaction rate between the ground state oxidized dye and Br^- plays a role in the overall kinetics (Eqn 6). Thermodynamically, it was expected that photocurrents would be enhanced at pH 1 where the conduction band (CB) of the metal-oxide semiconductors is at its most positive favoring excited state injection; however, the experimental results revealed the opposite. Analysis of bromine in the pH 5.6 solution with acetate buffer revealed a spectrum that closely matched the absorption and molar absorptivity for Br_3^-.[31] Further ^{1}H NMR analysis confirmed a shift in the CH_3-peak of acetate in D_2O in the presence of added bromine suggesting a reaction between Br_2 and acetate. The same reaction was not observed at pH 1 with perchloric acid (Figure S1).[32]

$$TiO_2(e^-)\text{-}\mathbf{RuP}^{3+} + Br^- \rightarrow TiO_2(e^-)\text{-}\mathbf{RuP}^{2+} + \tfrac{1}{2}\, Br_2 \quad k_{CAT} \quad (6)$$

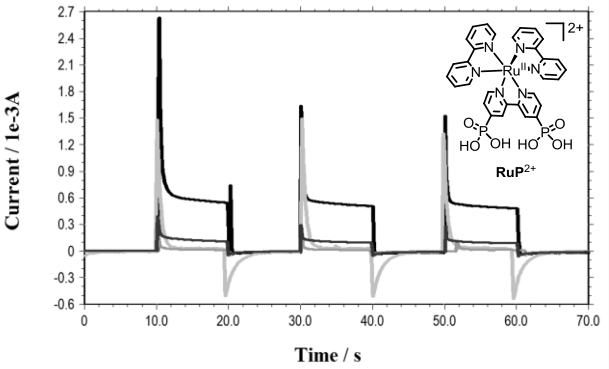

Figure 1. Current-time (i-t) traces for 0.5 cm^2 electrodes of TiO_2-**RuP**$^{2+}$ (light black) and SnO_2/TiO_2-**RuP**$^{2+}$ (black) in pH 5.6, 0.2 M acetate buffer, 0.25 M $NaClO_4$, and in pH 1, 0.1 M $HClO_4$ TiO_2-**RuP**$^{2+}$ (light gray) and SnO_2/TiO_2-**RuP**$^{2+}$ (gray); 40 mM LiBr, 100 mW/cm^2 illumination (white light source), E_{app} = 0.7 vs RHE.

To differentiate the formation of Br_3^- from Br_2 at pH 5.6, 18-crown-6 was added at pH 1 (0.1 M $HClO_4$) and unbuffered pH 7 (0.5 M $NaClO_4$) solutions of Br_2. The addition of 18-crown-6 to bromine under non-aqueous conditions has been known to initiate tribromide formation, Eqn 7.[33] Adding an equivalent of 18-crown-6 to Br_2 at pH 1 and 7 led to the formation of the Br_3^- spectrum and a loss of the Br_2 signal (Figure S2). The experimental results are consistent that, in a similar manner as 18-crown-6, acetate reacts with Br_2 to yield bromine acetate-tribromide, Eqn 8. The bromine acetate adduct, Br-O-C(O)CH_3, is a known complex which is often used in electrophilic halogenation of aromatic rings.[34]

$$2Br_2 + \text{18-crown-6} \rightarrow \text{18-crown-6-}Br^+\text{---}Br_3^- \quad (7)$$

$$2Br_2 + CH_3C(O)\text{-}O^- \rightarrow CH_3C(O)\text{-O-Br---}Br_3^- \quad (8)$$

Addition of 18-crown-6 to pH 1 solutions, with the same photocurrent measurements, resulted in a pronounced increase in photocurrent (Figure S3). Under 250 mW/cm^2 illumination the photocurrent density increased to 7 mA/cm^2. These results are remarkable and may be relevant for the development of aqueous DSSCs.[35]

Based on the improved photocurrent densities observed, it is likely that reduction of bromine acetate or the 18-crown-6 chelate are slower than bromine reduction at the photoanode. In the iodine/triiodide couple, which is ubiquituous in dye-sensitized solar cells (DSSCs), the major recombination pathway is through iodine (I_2).[36-39] The same appears to be true for bromine in aqueous solutions. Electrochemical measurements at pH 1, at pH 5.6 acetate buffer, and at pH 7 unbuffered solutions were consistent with the slowest step occurring in the acetate buffered solution using either a Pt or glassy carbon electrode evidenced by the larger peak separation (Figure S4). Long-term photo-electrolysis in pH 5.6, 0.2 M acetate buffer solution with a SnO_2/TiO_2-**RuP**$^{2+}$ electrode under white light illumination (100 mW/cm^2) for 20 min was carried out to determine the primary product of light-driven bromide oxidation. A sample of the photolysis solution was evaluated and bromine acetate or tribromide were the only product observed by UV-visible measurement.

To verify that the oxidized halogen intermediates could drive water oxidation by the [Ru(bda)(L)$_2$] catalysts, a series of experiments was carried out with [Ru(bda)(4-pic)$_2$] (pic = 4-

picoline) in solution.[19] Using either calcium hypochlorite ($Ca(ClO)_2$), hypobromous acid/hypobromite (HOBr/$^-$OBr) (prepared by adding $Ca(ClO)_2$ to a solution of 0.1 M Br^-), bromine, or tribromide as the oxidant. Sampling of the headspace by gas chromatography (GC) after ~5 min of mixing between the oxidants and catalyst confirmed, in all cases, quantitative conversion of the oxidative equivalents (~15-25 equiv.) into O_2 with 0.2 mM $[Ru(bda)(4\text{-pic})_2]$ in pH 5.6, 0.2 M acetate buffer solutions.[40]

Finally, assembling the SnO_2/TiO_2-**RuP**$^{2+}$ and performing long-term photolysis provided a solution of photogenerated bromine. After 30 min of illumination, an aliquot of a degassed pH 5.5 solution of **1** was added to the photochemical cell to form 0.05 mM **1** in solution. After 10 min of mixing, GC sampling of the headspace gave a 77% Faradaic efficiency for the production of O_2 based on the photocurrent measured at the SnO_2/TiO_2-**RuP**$^{2+}$ electrode and moles of evolved O_2 determined by GC analysis (Figure 2).

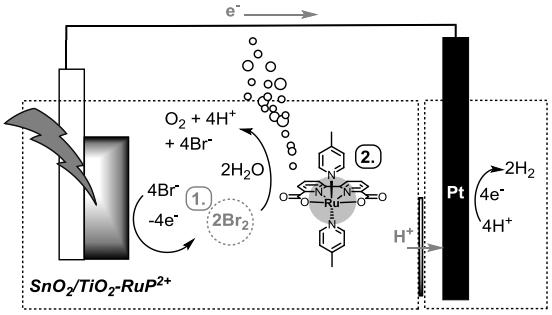

Scheme 2. DSPEC design based on using Br_2/Br^- or $[CH_3C(O)OBr\{Br_3\}]Na/Br^-$ redox mediator couples and a homogeneous catalyst.

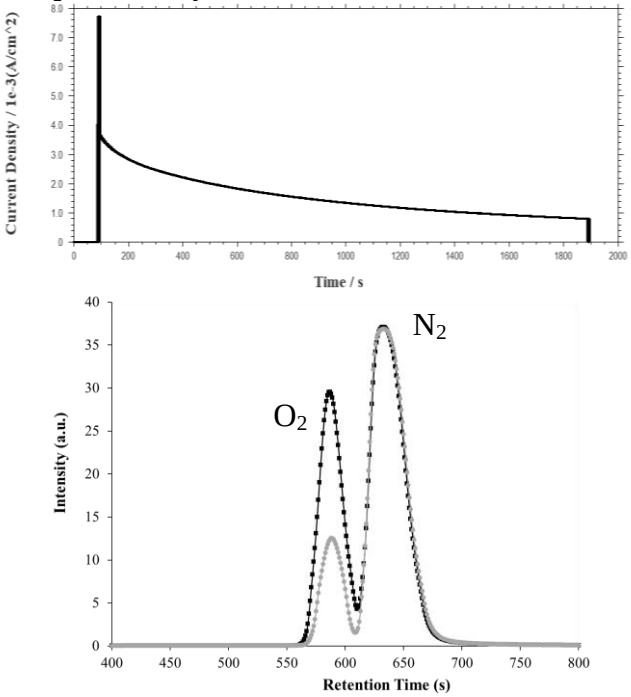

Figure 2. Photocurrent (top) and GC measurements (bottom) obtained for light-driven water splitting in pH 5.6 with 0.2 M acetate buffer and 40 mM LiBr and 40 mM 18-crown-6 at SnO_2/TiO_2-**RuP**$^{2+}$ photoanode (E_{app} = 0.7 V versus RHE) under 1 Sun illumination. GC measurements showing photolysis results in black with added **1** compared with a control experiment in gray for the same procedure run in the absence of the applied voltage and illumination.

In conclusion, the experiments described here establish the use of a bromide mediator couple that allows for light-driven water splitting upon addition of a homogeneous WOC. The approach exploits rapid, single e$^-$-based oxidation of the reduced mediator (Br^-) at the photoanode surface and removes high-valent forms of the catalyst from the reduced semiconductor surface. With relatively slow rates of recombination between the oxidized mediator and the reduced semiconductor surface, such as that observed with $[CH_3C(O)OBr\{Br_3\}]Na$ here, allows for buildup of oxidative equivalents in solution and subsequent water oxidation at **1**. The results described here could form the basis for the evolution of a new class of highly efficient photoanodes and enable the use of WOCs that hitherto have not performed well at metal-oxide semiconductor-dye interfaces such as nanoparticle metal oxides. Future experiments to develop a *nano*ITO mesoporous support containing $[Ru(bda)(4\text{-}PO_3H_2\text{-}(CH_2)_3\text{-pyr})_2]$ (pyr = pyridine),[30] in a configuration reminiscent of a collector-generator (C-G) cell, Scheme 3, are underway to establish an ideal configuration for continuous light-driven water splitting through a bromide-bromine mediator.[41]

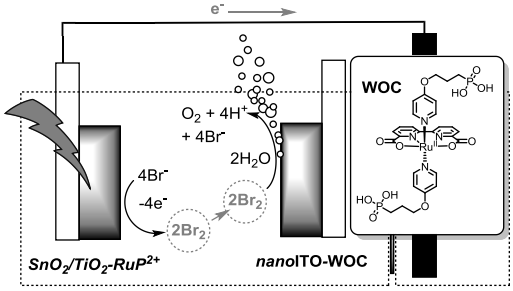

Scheme 3. DSPEC design based on using Br_2/Br^- or $[CH_3C(O)OBr\{Br_3\}]Na/Br^-$ redox mediator couples and a heterogeneous catalyst.

Acknowledgements

This research was solely supported by the UNC EFRC Center for Solar Fuels, an Energy Frontier Research Center funded by the U.S. Department of Energy, Office of Science, Office of Basic Energy Sciences, under Award No. DE-SC0001011, supporting studies on photoelectrochemical water splitting.

Keywords: photoelectrochemistry • photochemistry • water oxidation • water splitting • energy storage

[1] A. C. Nielander, M. R. Shaner, K. M. Papadantonakis, S. A. Francis, N. S. Lewis *Energy Environ. Sci.* **2015**, *8*, 16-25.
[2] S. Licht *J. Phys. Chem. B* **2003**, *107*, 4253-4260.
[3] A. Magnuson, M. Anderlund, O. Johansson, P. Lindblad, R. Lomoth, T. Polivka, S. Ott, K. Stensjö, S. Styring, V. Sundström, L. Hammarström *Acc. Chem. Res.* **2009**, *42*, 1899.
[4] J. D. Blakemore, R. H. Crabtree, G. W. Brudvig *Chem. Rev.* **2015**, *115*, 12974.
[5] C. C. L. McCrory, S. Jung, J. C. Peters, T. F. Jaramillo *J. Am. Chem. Soc.* **2013**, *135*, 16977.
[6] N. S. Lewis *Science , 351*, aad1920.
[7] C. J. Flynn, S. M. McCullough, E. Oh, L. Li, C. C. Mercado, B. H. Farnum, W. Li, C. L. Donley, W. You, A. J. Nozik, J. R.

McBride, T. J. Meyer, Y. Kanai, J. F. Cahoon *ACS Appl. Mater. Interfaces* **2016***, 8*, 4754-4761.
[8] T. J. Meyer *Nat. Chem.* **2011***, 3*, 757.
[9] L. Alibabaei, B. D. Sherman, M. R. Norris, M. K. Brennaman, T. J. Meyer *Proc. Natl. Acad. Sci. USA* **2015***, 112*, 5899-5902.
[10] B. H. Farnum, K. Wee, T. J. Meyer *Nat. Chem.* **2016***, 8*, 845-852.
[11] J. R. Swierk, K. P. Regan, J. Jiang, G. W. Brudvig, C. A. Schmuttenmaer *ACS Energy Lett.* **2016***, 1*, 603-606.
[12] R. R. Knauf, B. Kalanyan, G. N. Parsons, J. L. Dempsey *J. Phys. Chem. C* **2015***, 119*, 28353-28360.
[13] M. K. Gish, A. M. Lapides, M. K. Brennaman, J. L. Templeton, T. J. Meyer, J. M. Papanikolas *J. Phys. Chem. Lett.* **2016***, 7*, 5297-5301.
[14] N. S. McCool, J. R. Swierk, C. T. Nemes, C. A. Schmuttenmaer, T. E. Mallouk *J. Phys. Chem. Lett.* **2016***, 7*, 2930-2934.
[15] Benjamin D. Sherman, Dennis L. Ashford, Alexander M. Lapides, Matthew V. Sheridan, Kyung-Ryang Wee, Thomas J. Meyer *J. Phys. Chem. Lett.* **2015***, 6*, 3213-3217.
[16] M. V. Sheridan, B. D. Sherman, R. L. Coppo, D. Wang, S. L. Marquard, K. Wee, N. Y. Murakami Iha, T. J. Meyer *ACS Energy Lett.* **2016***, 1*, 231-236.
[17] T. Michalowski *J. Chem. Educ.* **1994***, 71*, 560.
[18] L. Duan, L. Wang, F. Li, F. Li, L. Sun *Acc. Chem. Res.* **2015***, 48*, 2084.
[19] L. Duan, F. Bozoglian, S. Mandal, B. Stewart, T. Privalov, A. Llobet, L. Sun *Nat. Chem.* **2012***, 4*, 418.
[20] N. Song, J. J. Concepcion, R. A. Binstead, J. A. Rudd, A. K. Vannucci, C. J. Dares, M. K. Coggins, T. J. Meyer *Proc. Natl. Acad. Sci. USA* **2015***, 112*, 4935-4940.
[21] Z. Chen, J. J. Concepcion, N. Song, T. J. Meyer *Chem. Commun.* **2014***, 50*, 8053-8056.
[22] P. Cettou, P. M. Robertson, N. Ibl *Electrochim. Acta* **1984***, 29*, 875-885.
[23] M. Mastragostino, C. Gramellini *Electrochim. Acta* **1985***, 30*, 373-380.
[24] D. A. Palmer, R. W. Ramette, R. E. Mesmer *J. Solution Chem.* **1984***, 13*, 673-683.
[25] G. D. Allen, M. C. Buzzeo, C. Villagrán, C. Hardacre, R. G. Compton *J. Electroanal. Chem.* **2005***, 575*, 311-320.
[26] G. Li, W. M. Ward, G. J. Meyer *J. Am. Chem. Soc.* **2015***, 137*, 8321-8323.
[27] K. Y. Tsai, I. Chang *Inorg. Chem.* **2017***, 56*, 8497-8503.
[28] K. Yun-Da, I-J. Chang *Inorg. Chem.* **2017***, 56*, 693.
[29] M. R. Norris, J. J. Concepcion, C. R. K. Glasson, Z. Fang, A. M. Lapides, D. L. Ashford, J. L. Templeton, T. J. Meyer *Inorg. Chem.* **2013***, 52*, 12492-12501.
[30] M. V. Sheridan, B. D. Sherman, K. Wee, S. L. Marquard, A. S. Gold, T. J. Meyer *Dalton Trans.* **2016***, 45*, 6324-6328.
[31] J. Xu, N. S. Georgescu, D. A. Scherson *J. Electrochem. Soc.* **2014***, 161*, H398.
[32] C. J. Schack, K. O. Christe, D. Pilipovich, R. D. Wilson *Inorg. Chem.* **1971***, 10*, 1078-1080.
[33] A. Semnani, H.R. Pouretedal, B. Nazari, A. Firooz *Sci. Iran.* **2003***, 10*, 317-321.
[34] I. Saikia, A. J. Borah, P. Phukan *Chem. Rev.* **2016***, 116*, 6837-7042.
[35] a) F. Bella, C. Gerbaldi, C. Barolo, M. Grätzel *Chem. Soc. Rev.* **2015***, 44*, 3431-3473; b) F. Bella, S. Galliano, M. Falco, G. Viscardi, C. Barolo, M. Grätzel, C. Gerbaldi *Green Chem.* **2017**, *19*, 1043-1051; c) C. Law, O. Moudam, S. Villarroya-Lidon, B. O'Regan *J. Mater. Chem.* **2012**, *22*, 23387-23394; d) S. Galliano, F. Bella, C. Gerbaldi, M. Falco, G. Viscardi, M. Grätzel, C. Barolo *Energy Technol.* **2017**, *5*, 300-311.
[36] G. Boschloo, A. Hagfeldt *Acc. Chem. Res.* **2009***, 42*, 1819-1826.
[37] B. A. Gregg, F. Pichot, S. Ferrere, C. L. Fields *J. Phys. Chem. B* **2001***, 105*, 1422-1429.
[38] A. Mathew, V. Anand, G. M. Rao, N. Munichandraiah *Electrochim. Acta* **2013***, 87*, 92-96.
[39] C. E. Richards, A. Y. Anderson, S. Martiniani, C. Law, B. C. O'Regan *J. Phys. Chem. Lett.* **2012***, 3*, 1980-1984.
[40] Using a Unisense probe to test for oxygen was unsuccessful. Gaseous chlorine or bromine led to a saturation in the signal at the detector.
[41] B. D. Sherman, M. V. Sheridan, C. J. Dares, T. J. Meyer *Anal. Chem.* **2016***, 88*, 7076-7082.

Entry for the Table of Contents (Please choose one layout)

Layout 1:

COMMUNICATION

Text for Table of Contents

((Insert TOC Graphic here))

*Author(s), Corresponding Author(s)**

Page No. – Page No.

Title

Layout 2:

COMMUNICATION

((Insert TOC Graphic here))

*Author(s), Corresponding Author(s)**

Page No. – Page No.

Title

Text for Table of Contents